JACC: CARDIOVASCULAR IMAGING VOL. 3, NO. 10, 2010

ISSN 1936-878X/$36.00
PUBLISHED BY ELSEVIER INC. DOI:10.1016/j.jcmg.2010.08.010

iLIGHTS

THE YEAR IN IMAGING

The Year in Coronary Artery Disease

Stephan Achenbach, MD,* Christopher M. Kramer, MD,† William A. Zoghbi, MD,‡ Vasken Dilsizian, MD§

Erlangen, Germany; Charlottesville, Virginia; Houston, Texas; and Baltimore, Maryland

Imaging plays a central role in the diagnosis and management of coronary artery disease. Imaging is used for the detection of underlying coronary artery stenoses in patients with stable or chronic chest pain, for the assessment of myocardial scar and viability, for assessing prognosis, or for predicting complications. Echocardiography, nuclear imaging, cardiac magnetic resonance, and—more recently—computed tomography are powerful tools to provide answers to these questions. New technology, new contrast agents, and newly developed imaging protocols widen the applicability and increase accuracy of these imaging modalities, and new clinical studies provide information on their diagnostic potential and their therapeutic as well as prognostic value. The relative strengths and weaknesses of the different imaging modalities influence the selection of the most appropriate imaging approach in different clinical scenarios. This article outlines some of the most important developments of the past 12 months in the field of echocardiography, nuclear imaging, cardiac magnetic resonance, and computed tomography as they pertain to coronary artery disease. (J Am Coll Cardiol Img 2010;3:1065–77) © 2010 by the American College of Cardiology Foundation

New Technology

In all areas of cardiac imaging, new novel technologies or imaging approaches might have substantial clinical impact when imaging conditions are difficult. Echocardiography for example might be hampered by low-quality images that would make accurate evaluation of ventricular function difficult, which in turn might lead to increased downstream use of other diagnostic modalities. The impact of contrast echocardiography on management in patients with technically difficult studies was evaluated prospectively in 632 patients (1). Improved endocardial visualization with contrast resulted in avoidance of additional diagnostic procedures in 32.8% and altered management in 10.4%. Advantages were highest in intensive care units (1). Similarly, global longitudinal strain, an automated technique for measuring percent myocardial shortening along the long axis of the left ventricle (LV), was evaluated at rest as an index of ventricular function in 546 patients and compared with

From the *Department of Cardiology, University of Erlangen, Erlangen, Germany; †Departments of Medicine and Radiology, University of Virginia Health System, Charlottesville, Virginia; ‡Department of Cardiology, The Methodist DeBakey Heart and Vascular Center, Houston, Texas; and the §Departments of Radiology and Medicine, University of Maryland School of Medicine, Baltimore, Maryland. Dr. Achenbach is partly supported by grant BMBF 01 EV 0708, from Bundesministerium für Bildung und Forschung, Bonn, Germany. He also has financial relationships with Siemens and Bayer Schering Pharma as a grant recipient and with Guerbet and Servier as a consultant. Dr. Kramer has financial relationships with Siemens Healthcare (research equipment support) and Astellas as a grant recipient. Dr. Dilsizian has financial relationships with Astellas, GE Healthcare, Lantheus, and Molecular Insight Pharma, Inc., as a consultant, advisory board, shareholder and/or grant recipient. Dr. Zoghbi reports that he has no relationships to disclose.

Manuscript received June 2, 2010; revised manuscript received July 27, 2010, accepted August 30, 2010.

JACC: CARDIOVASCULAR IMAGING, VOL. 3, NO. 10, 2010
OCTOBER 2010:1065–77

standard 2-dimensional echocardiography (2). Adding global longitudinal strain (hazard ratio [HR]: = 1.45) to clinical factors was more powerful in predicting cardiac events than wall motion score index (HR: = 1.28) or ejection fraction (HR: = 1.23). A global longitudinal strain cutoff of $>-12\%$ was equivalent to an ejection fraction of $<35\%$ in predicting prognosis.

Novel developments in 3-dimensional echocardiography include the application of speckle tracking to assess regional LV function. Seo et al. (3) validated LV strain measurements by 3-dimensional speckle tracking against data obtained by sonomicrometry in a sheep model of acute ischemia and pharmacologic stress. Good correlations were observed between noninvasive and invasive strain measurements (r range 0.84 to 0.90).

ABBREVIATIONS AND ACRONYMS

ACS = acute coronary syndrome

BMIPP = β-methyl-ρ-[123I]-iodophenyl-pentadecanoic acid

CABG = coronary artery bypass grafting

CAD = coronary artery disease

CFR = coronary flow reserve

CMR = cardiac magnetic resonance

CT = computed tomography

ECG = electrocardiogram

HR = hazard ratio

LGE = late gadolinium enhancement

LV = left ventricle/ventricular

MACE = major adverse cardiac events

MR = magnetic resonance

PCI = percutaneous coronary intervention

PET = positron emission tomography

SPECT = single-photon emission computed tomography

New data have become available concerning imaging of "ischemic memory" through nuclear medicine. After a transient ischemic event, persistent metabolic disturbances in fatty acid metabolism can occur for up to 30 h—termed "ischemic memory" (4). Radioiodine-labeled branched-chain fatty acid β-methyl-ρ-[123I]-iodophenyl-pentadecanoic acid (BMIPP) allows assessment of fatty acid metabolism with single-photon emission computed tomography (SPECT). In a recent multicenter trial, 448 emergency department patients with suspected acute coronary syndrome (ACS) were enrolled at 50 centers (5). Patients were imaged with BMIPP within 30 h of symptom cessation. Compared with initial clinical diagnosis alone, the combination of BMIPP with initial clinical diagnosis increased sensitivity for identifying patients with ACS from 43% to 81% ($p < 0.001$), negative predictive value from 62% to 83% ($p < 0.001$), and positive predictive value from 41% to 58% ($p < 0.001$), while maintaining specificity (61% to 62%, p = NS) (Fig. 1).

Another new tracer to study myocardial perfusion with positron emission tomography (PET) is an F-18 labeled pyridazone derivate, F-18 BMS. Because of the short physical half-life of rubidium-82 (75 s), stress myocardial perfusion rubidium PET studies are commonly performed with a pharmacologic vasodilator rather than exercise. The longer half-life of F-18 BMS (110 min) would allow its application as a perfusion agent during treadmill exercise as well as widen the clinical application of cardiac PET by allowing a single-dose unit distribution on a daily basis. In a porcine model of transient ischemia, myocardial uptake of F-18 BMS was compared with N-13 ammonia and radioactive microspheres (6). There was a relatively good correlation between the extent of myocardial perfusion defects measured by F-18 BMS and microspheres (r = 0.63, slope = 1.1) (7). Uptake ratios of myocardium-to-blood, myocardium-to-lung, and blood-to-liver were up to 3-fold higher for F-18 BMS than N-13 ammonia.

New contrast agents have also been evaluated for magnetic resonance (MR) imaging. A new collagen binding gadolinium-based contrast agent was tested in a porcine model of myocardial ischemia and shown to accurately assess perfusion defects (8). An albumin-bound gadolinium-based intravascular contrast agent was approved by the U.S. Food and Drug Administration for human use in peripheral MR angiography after pilot studies for whole-heart MR coronary angiography at 3.0-T were promising (9). Stronger magnetic fields might improve MR imaging. The first feasibility studies of cardiac imaging in humans on whole body 7.0-T MR scanners have been performed with fairly basic pulse sequences and promising initial results (10).

In X-ray computed tomography (CT) imaging, hardware specifications continue to improve. First clinical results of 320-slice scanners—albeit in small patient groups—have become available and indicate high diagnostic accuracy (11,12). In 64 patients, a recent study performed by 320-slice CT demonstrated a per-patient sensitivity of 100% and specificity of 88% for the identification of individuals with at least 1 stenosis >50%. Especially for patients with low heart rates, limiting data acquisition to 1 single cardiac cycle allowed achievement of low radiation exposure (with a mean estimated effective dose of 3.9 ± 1.3 mSv for heart rates <60 beats/min) (12). With a recently introduced second-generation dual source CT system, providing both increased detector coverage and rotation speed as compared with first-generation dual source CT, a new data acquisition mode has become possible for coronary CT angiography. Prospectively, electrocardiogram (ECG)-triggered spiral acquisition with high pitch values allows extremely low radiation doses. It has so far only been evaluated in small series of selected patients (13–16). In a series of 50 patients with suspected coronary artery disease (CAD), a heart rate below 60 beats/min and a body weight below 100 kg, an effective dose below 1.0

mSv was consistently achieved (mean dose: 0.87 ± 0.07 mSv) (Fig. 2) (17).

Diagnosis of CAD

Assessment of "diastolic stunning" might be a new approach to detect ischemia in echocardiography. Ishii et al. (18) evaluated whether post-ischemic delayed LV relaxation could be detected with strain imaging from 2-dimensional speckle-tracking echocardiography. Changes in regional LV strain during the first third of diastole were determined in 162 patients with effort angina. Ten minutes after exercise, regional delayed relaxation was still observed in 85% of ischemic territories (Fig. 3). A strain imaging diastolic index ratio had a sensitivity of 97% and a specificity of 93% to detect significant coronary stenosis (18).

A recent study evaluated the detection of CAD with perfusion stress dipyridamole echocardiography with a novel ultrasound imaging agent (Imagify, Acusphere, Cambridge, Massachusetts) in comparison with radionuclide perfusion imaging. Real-time Assessment of Myocardial Perfusion 1 and 2 were international, phase 3 trials in 662 patients. Accuracy for perfusion stress echo (66% to 71%) was noninferior to SPECT (67% to 70%) (Fig. 4) (19).

The strength and basis of nuclear imaging is the assessment of heterogeneity in myocardial perfusion at rest and during hyperemic flow. As opposed to visual or semi-quantitative interpretation of relative regional radiotracer uptake where the myocardial region with highest uptake is considered normal, PET myocardial perfusion imaging allows for the assessment of absolute myocardial blood flow in ml/min/g. In a recent publication (20), it was hypothesized that absolute measurement of myocardial blood flow (ml/min/g) by 13N-ammonia PET is superior to relative measurement of myocardial tracer retention (nCi/ml) for identification of CAD (≥70% diameter stenosis). In 48 subjects, the authors demonstrated that "single" adenosine vasodilator stress-stimulated PET measurement of absolute myocardial blood flow was all that was needed to attain sensitivity, specificity, and accuracies of 81%, 85%, and 84%, respectively, for detecting CAD. When myocardial blood flow reserve of less than 2-fold increase in adenosine-induced myocardial blood flow from rest was used (2 sets of

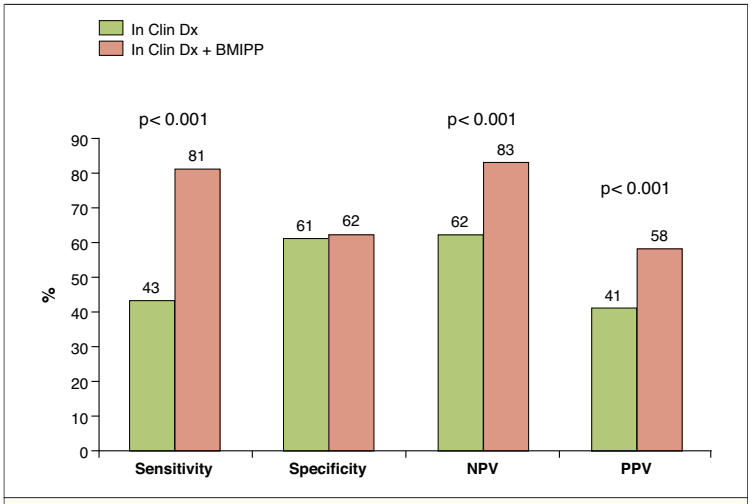

Figure 1. Incremental Value of BMIPP SPECT to Initial Clinical Information in Emergency Department for Early Diagnosis of Acute Coronary Syndromes

Performance characteristics for the initial clinical diagnosis (In Clin Dx) alone and the combination of the initial clinical diagnosis and β-methyl-ρ-[123I]-iodophenyl-pentadecanoic acid (BMIPP) single-photon emission computed tomography (SPECT) imaging are shown. The combination of BMIPP SPECT with initial clinical information resulted in improved sensitivity for identifying patients with acute coronary syndrome compared with the sensitivity of the In Clin Dx alone, while maintaining specificity. NPV = negative predictive value; PPV = positive predictive value. Reprinted, with permission, from Kontos et al. (5).

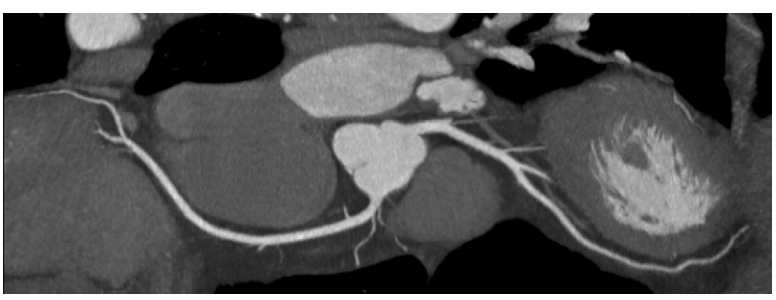

Figure 2. Very Low-Dose Coronary CT Angiography With Prospective Electrocardiogram-Triggered High-Pitch Spiral Acquisition With a Dual Source CT System

A multiplanar reconstruction of the right coronary artery, left main, and left anterior descending coronary artery is shown. The dose length product of this computed tomography (CT) angiography investigation was 47 cm*mGy, corresponding to an estimated effective dose of 0.7 mSv.

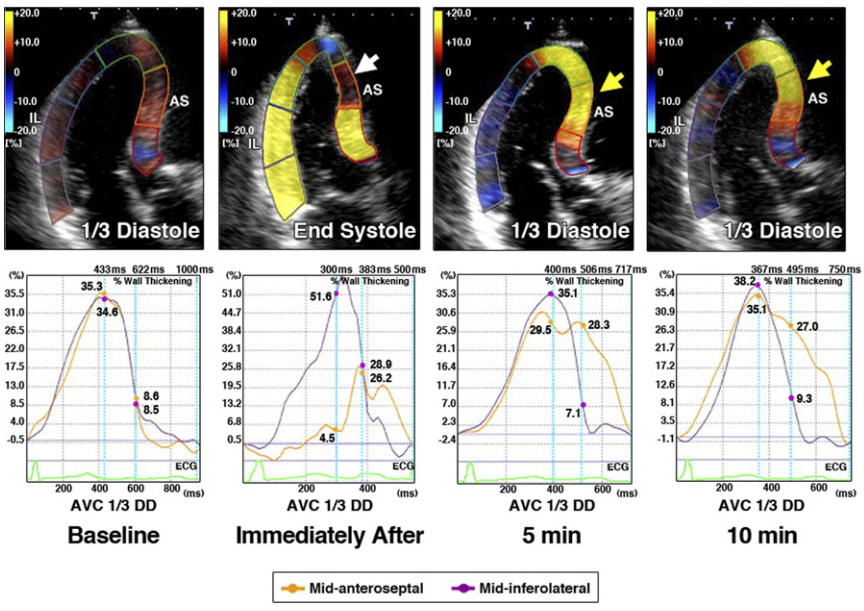

Figure 3. 2D Speckle Tracking Images and Transverse Strain Curves

The 2-dimensional (2D) speckle tracking images in the apical long-axis view **(top)** and transverse strain curves in mid-anteroseptal **(orange curve)** and mid-inferolateral **(purple curve)** segments **(bottom)**, obtained from a 68-year-old male patient with 70% coronary stenosis in segment 7 of the left anterior descending coronary artery at baseline, immediately after and 5 and 10 min after the treadmill exercise. **Top:** The color bar of strain is set as yellow according to increasing strain value. Immediately after exercise, a significant decrease of peak systolic strain developed in the mid-anteroseptal segment **(white arrow)**. Five minutes after exercise, the high strain level or yellow mapping area **(yellow arrow)** appeared in the mid-anteroseptal segment at one-third diastole duration, because of post-ischemic delayed reaction. After 10 min, the yellow mapping area has faded out but is still present in the mid-anteroseptal and apical segments at one-third duration. **Bottom:** At baseline, the strain imaging (SI)-diastolic index was 76% in the mid-anteroseptal segment. The index decreased to 4% 5 min after exercise and improved but remained depressed (23%) 10 min after exercise in the anteroseptal segment. No apparent changes of SI-diastolic index were observed during the follow-up period in the mid-inferolateral segment. 1/3 DD = one-third diastole duration; 5 min = 5 min after treadmill exercise; 10 min = 10 min after treadmill exercise; AS = mid-anteroseptal; AVC = aortic valve closure; IL = mid-inferolateral. Reprinted, with permission, from Ishii et al. (18).

images), the sensitivity, specificity, and accuracies were 62%, 85%, and 79%, respectively. When relative radiotracer uptake of <70% (normalized to peak normal reference region) was used, the sensitivity, specificity, and accuracies were 48%, 82%, and 72%, respectively. Hence, absolute myocardial blood flow on "single" adenosine PET images showed improved sensitivity without decreasing specificity, which might simplify clinical PET myocardial perfusion imaging for evaluation of patients with known or suspected CAD (20,21).

New nuclear cameras might also translate into better diagnosis of CAD. In a prospective, multicenter clinical trial of 238 patients, the authors used quantitative analysis to compare the ability of high-speed SPECT (which acquired images in one-seventh of the time) with that of conventional SPECT in detecting myocardial perfusion abnormalities (22,23). High-speed stress and rest total perfusion deficit correlated linearly with conventional SPECT ($r = 0.95$ and $r = 0.97$, respectively, $p < 0.0001$). Post-stress ejection fraction and end-diastolic volume by the 2 methods were linearly correlated ($r = 0.89$ and $r = 0.97$, respectively). Thus, high-speed SPECT measures of myocardial perfusion and function are comparable to those with conventional SPECT, with imaging completed in 2 to 4 min (23,24).

Data on the excellent accuracy of cardiac magnetic resonance (CMR) perfusion imaging for identification of ischemia continue to accumulate. In a study of 103 patients who underwent invasive measurement of fractional flow reserve, the sensitivity and specificity of CMR first-pass contrast-enhanced perfusion was 91% and 94%, respectively (25). In patients with prior percutaneous coronary intervention (PCI) or coronary artery bypass grafting (CABG) who had been typically excluded from prior studies of this kind, the combined use of perfusion imaging and late gadolinium enhancement (LGE) performed well to identify post-PCI patients with coronary stenoses (sensitivity 91%

and specificity 90%), although it was less accurate post-CABG (sensitivity 79%, specificity 77%) (Fig. 5) (26).

Noninvasive coronary angiography continues to increase in robustness. In a single-center study of patients with a mean body mass index of 24 kg/m^2, MR coronary angiography on a 3.0-T scanner displayed an accuracy of 84% (27). Increasing clinical data become available for CT coronary angiography. In 1,226 patients who underwent clinically driven coronary CT angiography to rule out coronary artery stenoses and who were followed for 18 months, Hadamitzky et al. (28) showed that there were only 4 events (1 unstable angina, and 3 revascularizations) in 802 individuals without obstructive coronary disease in CT, as compared with 17 events (1 nonfatal infarction, 4 unstable angina with a total of 15 revascularization procedures) in patients with at least 1 stenosis seen in CT angiography (Fig. 6). Chow et al. (29) demonstrated that, in 2,006 prospectively enrolled patients with suspected CAD but a normal CT scan, the annual event rate was only 0.26% (as compared with 10.5% for patients with stenoses in 3 or more coronary arteries). In 368 patients with acute chest pain, the ROMICAT (Rule Out Myocardial Infarction using Computer Assisted Tomography) trial confirmed a high sensitivity of coronary CT angiography to identify patients with acute coronary syndromes among those who present with normal troponin and absence of ischemic ECG changes (30). The presence of atherosclerosis on CT angiography had 100% sensitivity for the identification of patients with an acute coronary syndrome. Hollander et al. (31) demonstrated that, among 481 patients who had been admitted to the emergency room with chest pain and a low to intermediate likelihood of CAD but who were discharged on the basis of a "negative" coronary CT angiogram (no stenoses of 50% or more), event rates in the following year were very low: 53 patients (11%) had a repeat hospital stay, and 51 (11%) received further diagnostic testing, but there was no acute coronary syndrome, no revascularization, and only 1 death (0.2%) of unclear etiology.

Coronary CT angiography visualizes anatomy, whereas most other noninvasive tests for CAD rely on ischemia, and the relationship between the 2 has been tested in numerous trials. Min et al. (32) published a thorough review of the potential role of coronary CT angiography and clearly summarized that the presence of coronary artery stenoses in CT angiography has a low positive predictive value for the presence of inducible ischemia (29% to 44%), whereas the negative predictive value was high in all published studies (88% to 100%). Hence, CT angiography is likely a good test to rule out CAD but not a sufficient test to base revascularization on. In fact, the effectiveness of a given test to work up patients with suspected CAD not only depends on test characteristics (sensitivity, specificity) but also depends substantially on the pre-test likelihood of disease, which in turn influences the positive predictive value. In some clinical situations, anatomic imaging (coronary CT angiography) might be more cost-effective than imaging for ischemia. A number of recent trials have investigated this issue and found coronary CT angiography cost-effective, es-

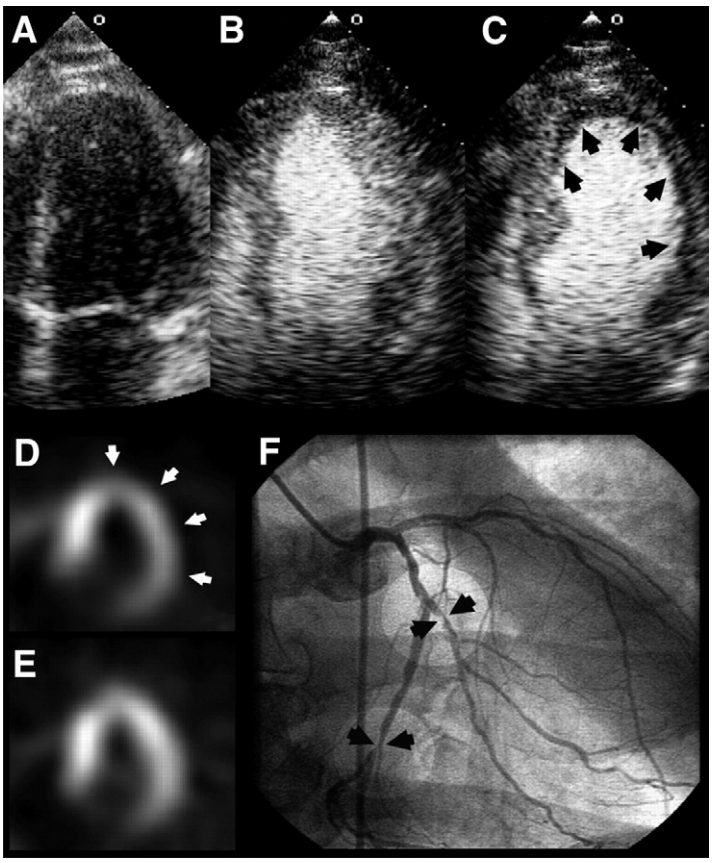

Figure 4. Detection of Coronary Artery Disease by Perfusion Stress Echocardiography

Apical 4-chamber view without contrast and after administration of Imagify at rest **(A, B)**. Apical lateral (inducible subendocardial) perfusion defect during perfusion stress echocardiography **(C)**, corresponding to a similar perfusion defect on horizontal long-axis view in stress single-photon emission computed tomography **(D)**. Single-photon emission computed tomography image at rest **(E)**. Coronary angiography with lesions in left circumflex system **(F)**. Images were obtained from the same patient at rest and with dipyridamole. **Black arrows** indicate subendocardium **(C)**. **White arrows** indicate perfusion defects **(C, D)** and angiographic lesions **(F)**. Reprinted, with permission, from Senior et al. (19).

JACC: CARDIOVASCULAR IMAGING, VOL. 3, NO. 10, 2010
OCTOBER 2010:1065–77

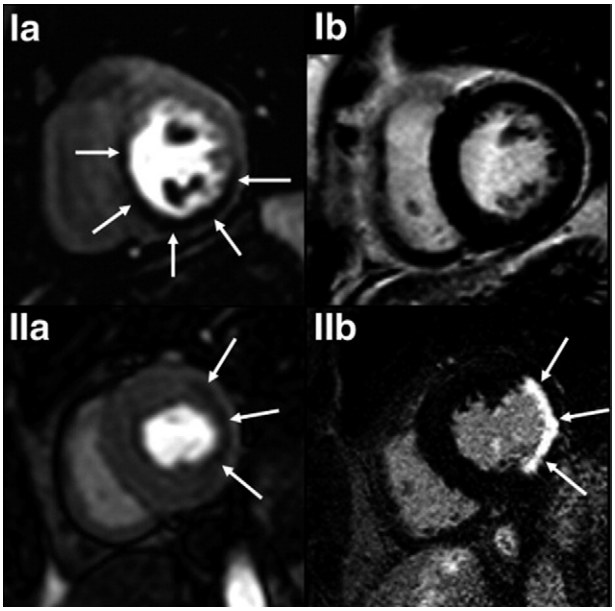

Figure 5. CMR for Detection of Myocardial Ischemia in a Post-Revascularization Patient

Adenosine stress perfusion cardiac magnetic resonance (CMR) images in a patient after coronary artery bypass graft surgery with corresponding late gadolinium enhanced (LGE) images. Adenosine-stress perfusion CMR image **(Ia)** showing perfusion defect of the inferior and inferoseptal myocardial wall **(arrows)** in the absence of LGE **(Ib)**. Perfusion deficit of the lateral wall **(IIa, arrows)** during adenosine with corresponding presence of LGE **(IIb, arrows)**. The subendocardial low signal intensity in the left anterior descending and right coronary artery perfusion areas was not regarded as significant perfusion deficit but as dark rim artifact. Reprinted, with permission, from Bernhardt et al. (26).

pecially when pre-test likelihood was low or intermediate. Similarly, coronary CT angiography was found to be cost-effective in acute chest pain patients (33–37).

A new approach to identifying the presence and severity of CAD by CT imaging is the assessment of myocardial hypoperfusion at rest in acute coronary syndromes (38) or during pharmacologic stress (Fig. 7). Several recent publications indicated the ability of contrast-enhanced CT imaging under stress to visualize myocardial hypoperfusion and found close correlation to other tests for ischemia, such as SPECT (39–42); 1 study could demonstrate an enhanced accuracy of CT for the detection of coronary stenoses when combining CT angiography with CT myocardial perfusion imaging. The studies were small, but results are compelling enough to conduct larger clinical trials.

Imaging of Infarct Size and Viability

Cardiac MR has long been recognized for its ability to detect scars after myocardial infarction through late gadolinium enhancement (LGE) (43). In addition to clinical work, LGE CMR is being increasingly used in clinical trials to measure effects of novel medical therapies such as cyclosporine (44), FX06—a naturally occurring fibrin-derived peptide (45)—as well as interventional therapies such as ischemic post-conditioning during primary PCI (46). Old infarcts show transformation into lipid tissue, and an analysis of 53 patients with past myocardial infarction showed that 89% of patients with an infarct age of 3 years or more had detectable fatty deposits in the LV wall in CT imaging (47). It has recently been recognized that CMR, next to "late enhancement," also allows imaging of myocardial edema in the acute setting with T2-weighted imaging. In vivo studies using T2-weighted measurement of myocardium at risk showed that the mean time for final infarct size to reach 50% of the area at risk in humans is 288 min (48).

In echocardiography, strain imaging can provide information on viability. Longitudinal strain imaging from speckle tracking echocardiography was used to identify viable myocardium in 90 patients with chronic ischemic LV dysfunction (49). A regional strain value of −4.5% discriminated between segments with viable myocardium and those with transmural scar with a sensitivity of 81.2% and specificity of 81.6% (49).

Prognosis/Risk Stratification

Various imaging methods use different strategies to assess the risk of future cardiovascular events. Echocardiography mainly assesses wall motion, SPECT and PET are targeted at myocardial perfusion, MR imaging is used to detect infarct scars, and CT attempts to image the culprit itself, atherosclerotic lesions in the coronary artery tree.

The prognostic value of peak and post-exercise treadmill echocardiography was evaluated in 2,947 patients (50). Although post-exercise imaging with derivation of wall motion score was predictive of major cardiac events, imaging at peak exercise was additive as it detected patients with ischemia that were not identified after exercise (50). Another study from the same institution (51) evaluated the incremental value of echocardiographic imaging in patients with normal stress ECG undergoing treadmill stress. In 4,004 patients, ischemia on stress echocardiography more than doubled the rate of cardiac death or myocardial infarction during the following 5 years, whereas a normal stress echocardiogram predicted a low yearly event rate of 0.64%

in those who also had a normal resting echocardiogram (51).

In another study, global strain rate was a powerful and independent predictor (HR = 2.16) of all-cause mortality in individuals undergoing dobutamine stress echocardiography and provided incremental information over baseline clinical and echocardiographic variables (52). Among LV geometric patterns, concentric hypertrophy had the worst outcome.

Myocardial perfusion imaging has long been recognized to have substantial prognostic value. New data illustrate that, besides predicting mortality and infarcts, myocardial perfusion SPECT might also predict heart failure (53). In a multicenter, prospective, observational study of 3,835 CAD patients undergoing stress myocardial perfusion SPECT, 71 (1.8%) developed new-onset heart failure over 3 years (54). Renal dysfunction, end-systolic volume index, and large stress perfusion defect were independent predictors of heart failure, and the combination of the 3 had the greatest incremental prognostic value (Fig. 8). Whether early aggressive therapy can modify the risk for developing HF in these patients is an important study to undertake next.

To date, prognostic studies with myocardial perfusion SPECT in elderly populations are limited. Although elderly persons constitute only 6.1% of the U.S. population, they suffer two-thirds of all cardiovascular deaths. Patients ≥75 years of age (n = 5,200) were followed for a mean of 2.8 years after myocardial perfusion scintigraphy (55). Both SPECT-measured ischemia and fixed defects added incrementally to pre-SPECT data. Among the 684-patient subgroup who had an extended mean follow-up period of 6.2 years, an interaction between early treatment and myocardial ischemia by SPECT was present; increasing ischemia was associated with increasing survival with early revascularization, whereas in the setting of little or no ischemia, medical therapy had improved outcomes (55). It has to be noted that this report did not randomize patients to medical treatment versus revascularization and the reason for impaired survival with early revascularization is not known.

As an alternative strategy to traditional rest-stress SPECT protocols, a recent study advocates performing the stress study first (56). Rest imaging is performed only if the stress study is equivocal or clearly abnormal. Accordingly, all-cause mortality was assessed in 16,854 consecutive patients who had a normal gated stress SPECT; 8,034 (47.6%) were studied with stress-only protocol, and 8,820 (52.4%) had both stress and rest imaging. Over a median follow-up period of 4.5 years, the overall unadjusted annual mortality rate in patients who had a normal SPECT with a stress-only protocol was lower than in those who required additional rest imaging (2.57% vs. 2.92%, p = 0.02). No significant differences in adjusted patient mortality were seen between the 2 imaging protocols, but the stress-only group received a 61% lower radiopharmaceutical dose (56), which supports the notion that additional rest imaging is not required in a selected group of patients with normal initial stress myocardial perfusion SPECT.

As compared with SPECT, PET has higher diagnostic accuracy for detecting CAD (owing to better resolution, attenuation correction, and higher energy radiotracers) and might be a better predictor of events. In 229 patients with suspected myocardial ischemia who underwent 13N-ammonia PET, the long-term prognostic value of coronary flow reserve (CFR) was assessed over a mean of 5.4 years (57). Major adverse cardiac events (MACE), including 29 cardiac deaths, occurred in 78 (34%) patients. Abnormal PET perfusion (n = 126) was associated with a higher incidence of MACE ($p < 0.001$) and cardiac death ($p < 0.05$). In patients with normal perfusion, abnormal CFR was independently asso-

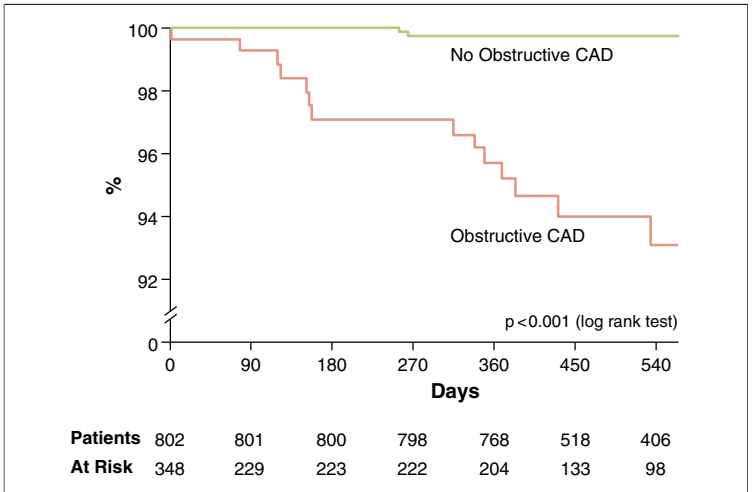

Figure 6. Prognostic Value of CT Coronary Angiography

Kaplan-Meier curve for cardiac events in 1,256 patients investigated by coronary computed tomography (CT) angiography. Cardiac events are defined as cardiac death, nonfatal myocardial infarction, unstable angina requiring hospital stay, or coronary revascularization later than 90 days after coronary CT angiography. The event rate for patients without obstructive coronary artery disease (CAD) **(green line)** was 0.25%; for patients with obstructive CAD **(brown line),** it was 4.3% (odds ratio: 16.1, 95% confidence interval: 7.2 to 36.0). Reprinted, with permission, from Hadamitzky et al. (28).

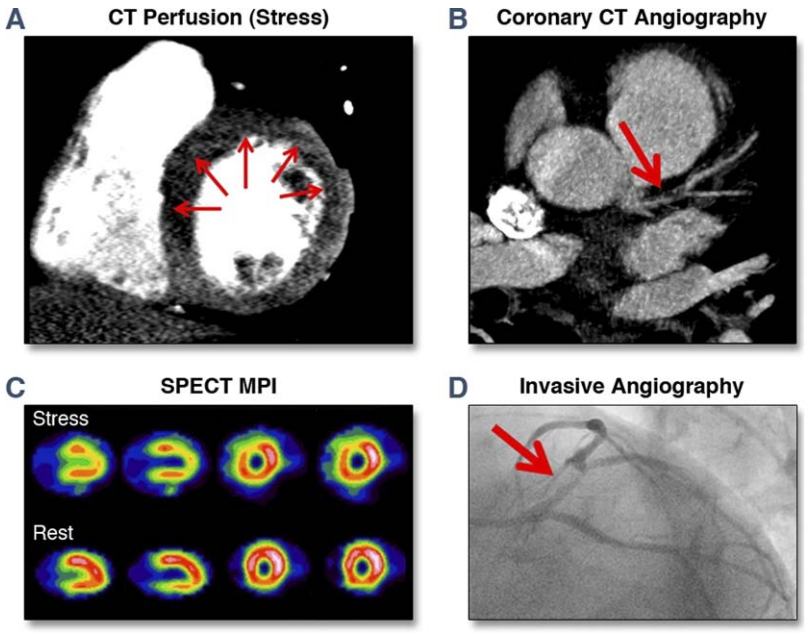

Figure 7. Example of Single-Vessel Disease Identified by Stress CT MPI

A 59-year-old obese man with no prior cardiac history who presented with chest pain and dyspnea on exertion. Computed tomography (CT) perfusion showed a large perfusion defect in the anteroseptal, anterior, and anterolateral walls **(A)**. **(B)** CT angiography showed large noncalcified plaque in the proximal left anterior descending coronary artery (LAD); **(C)** single-photon emission computed tomography (SPECT) myocardial perfusion imaging (MPI) images with fully reversible defect throughout the mid and apical anterior wall. **(D)** Invasive angiography in the left anterior oblique caudal view showing severe stenosis in LAD before the takeoff of the first diagonal branch. Reprinted, with permission, from Blankstein et al. (39).

ciated with a higher annual event rate over 3 years for MACE (1.4% vs. 6.3%; $p < 0.05$) and cardiac death (0.5% vs. 3.1%; $p < 0.05$) as compared with normal CFR. In patients exhibiting abnormal perfusion, CFR remained predictive throughout the 10-year follow-up ($p < 0.001$). Hence, abnormal CFR in ^{13}N-ammonia PET is an independent predictor of adverse outcome (58) (Fig. 9).

Late gadolinium enhancement CMR provides prognostic information, beyond other measures of risk, and more data have become available (59,60). A study of 349 patients with severe ischemic cardiomyopathy and mean LV ejection fraction of 24% demonstrated that a greater semiquantitative measure of scar by LGE was associated with higher mortality or need for cardiac transplantation (61). Patients with new scars as detected by LGE after a revascularization procedure were shown to have a 3.1-fold greater risk of adverse outcomes compared with those without new scars, whereas troponin levels and ejection fraction had no predictive value (62).

Imaging of coronary artery calcification has been the mainstay of risk stratification by CT. Recently published data in large patient cohorts support the strong prognostic power of coronary calcium measurements in asymptomatic individuals (63–65). Min et al. (66) addressed an interesting question in a study that included 422 individuals (mean age 47 years) who had a calcium score of 0 (absence of calcium): what is the "warranty period" of a 0 calcium scan? The group was followed for a period of 5 years by annual CT scans for coronary calcium. The authors documented conversion from 0 calcium scores to detectable calcium in 2, 5, 24, 26, and 49 individuals in follow-up years 1, 2, 3, 4, and 5, with a mean time to conversion of 4.1 years. Age, diabetes, and smoking were independent predictors of conversion. The authors conclude that there is a very low rate of conversion to positive calcium score up to 4 years (indeed, much of the early conversions can probably be explained by the less-than-perfect reproducibility of coronary calcium scans) and that during this time period repeat calcium scanning is not warranted. Whether coronary CT angiography, by documenting noncalcified plaque, might have additional prognostic value beyond coronary calcium has been much debated. The question was addressed in a cohort of 423 mostly symptomatic individuals who underwent clinically indicated cor-

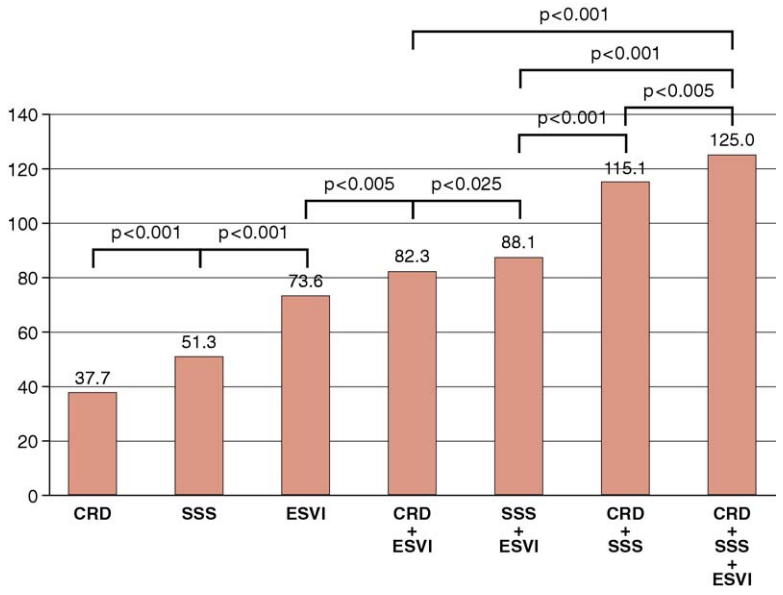

Figure 8. Global Chi-Square Values for Predicting New-Onset Refractory HF in a Study of 3,835 Patients With Coronary Artery Disease

Global chi-square values for predicting new-onset refractory heart failure significantly and incrementally increase when chronic renal dysfunction (CRD), end-systolic volume index (ESVI), and summed stress score (SSS) in myocardial perfusion single-photon emission computed tomography (SPECT), all of which were determined by multivariable Cox analysis, are combined. Reprinted, with permission, from Nakata et al. (54).

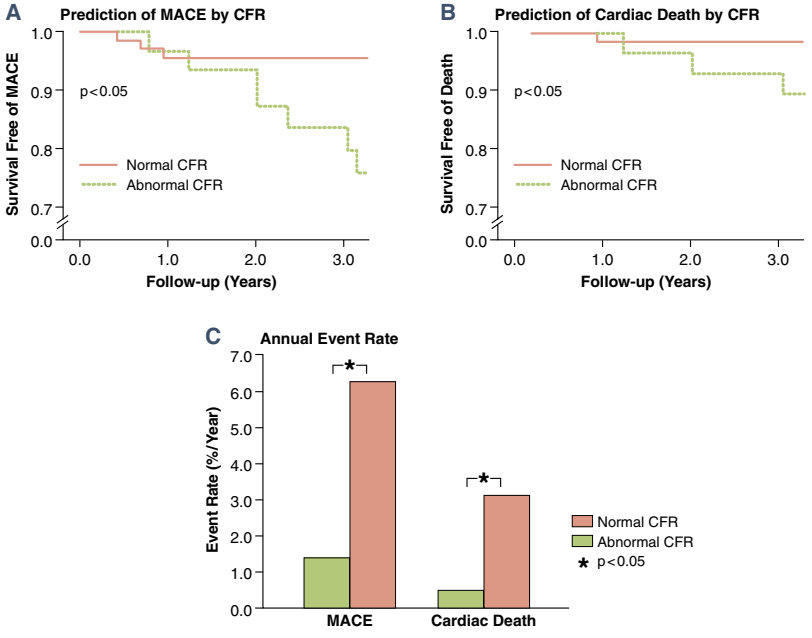

Figure 9. Predictive Value of CFR Measured by ^{13}N-ammonia PET

Coronary flow reserve (CFR) is an independent predictor of adverse outcome. It provides a 3-year "warranty" period of event-free survival for patients with normal CFR and normal positron emission tomography (PET) perfusion (3-year follow-up). Abnormal CFR predicts adverse outcome, that is, major adverse cardiac event (MACE) **(A)** and cardiac death **(B)**, despite normal perfusion. This is reflected by the higher annual event rate (%/year) in abnormal CFR **(C)**. Reprinted, with permission, from Dilsizian et al. (58).

onary CT angiography and were then followed for a median period of 670 days (67). Twenty-one patients experienced an event (6 deaths, myocardial infarction in 8 patients, and unstable angina requiring revascularization in 7 patients). After adjustment for calcium scores (threshold: calcium score 1,000), the presence of any stenosis ≥50%, the number of diseased coronary artery segments, the number of segments with obstructive plaque, and the presence of noncalcified plaque were independent predictors of events. Thus, the authors conclude that CT angiography has prognostic value independent of the calcium score. Although the reported calcium cutoff (score of 1,000) seems high, the authors reported in a personal communication that using lower calcium score thresholds yielded the same results. Another study that highlighted the potential of CT to detect and analyze noncalcified plaque was published by Uetani et al. (68), in a different context. They imaged 189 patients scheduled for elective revascularization by contrast-enhanced 64-slice CT and measured the volume of plaque in the culprit lesion. They could show that the total volume of atherosclerotic plaque in the target lesion measured by CT as well as the volume of plaque with low CT attenuation (below 50 Hounsfield units and below 150 Hounsfield units, respectively) correlated with the occurrence of peri-procedural myocardial infarction as detected by a troponin increase.

A new measure of cardiovascular risk might be the amount of pericardial fat, which can easily be measured from nonenhanced CT scans. Cheng et al. (69) used automated measurements of pericardial fat burden to predict cardiac death, infarction, stroke, and late revascularization in a cohort of 2,751 asymptomatic individuals. They found a higher mean pericardial fat volume in 58 patients with events as compared with patients without events (102 ± 49 cm^2 vs. 85 ± 38 cm^2, $p = 0.007$), even after adjusting for risk factors and the presence of coronary calcium.

New Guidelines and Recommendations

Recognizing the importance of high procedural quality in imaging, several societies published guidelines on data acquisition and interpretation in cardiac imaging. The American Society of Nuclear Cardiology published "Imaging Guidelines for Nuclear Cardiology Procedures: PET myocardial perfusion and metabolism clinical imaging" (58), and the Society of Cardiovascular Computed Tomography published recommendations for data acquisition and reporting of coronary CT angiography in 2 separate documents (70,71). Similarly, the Society for Cardiovascular Magnetic Resonance published new guidelines for reporting CMR examinations in a comprehensive manner (72). Regarding clinical indications for cardiac CT and CMR, 2 very recent Expert Consensus Documents have become available (73,74). "Appropriate Use Criteria" for cardiac radionuclide imaging have been published (75) and an update of the "Appropriateness Criteria" for cardiac CT is expected very soon.

Reprint requests and correspondence: Dr. Stephan Achenbach, Department of Internal Medicine II (Cardiology), University of Erlangen, Ulmenweg 18, Erlangen 91054, Germany. *E-mail: stephan.achenbach@uk-erlangen.de.*

REFERENCES

1. Kurt M. Shaikh KA, Peterson L, et al. Impact of contrast echocardiography on evaluation of ventricular function and clinical management in a large prospective cohort. J Am Col Cardiol 2009;53:802–10.
2. Stanton T, Leano R, Marwick T. Prediction of all-cause mortality from global longitudinal speckle strain: comparison with ejection fraction and wall motion scoring. Circ Cardiovasc Img 2009;2:356–64.
3. Seo Y, Ishizu SY, Enomoto Y et al. Validation of 3-dimensional speckle tracking imaging to quantify regional myocardial deformation. Circ Cardiovasc Imaging 2009;2:451–9.
4. Dilsizian V, Bateman TM, Bergmann SR, et al. Metabolic imaging with β-methyl-ρ-[123I]-iodophenyl-pentadecanoic acid (BMIPP) identifies ischemic memory following demand ischemia. Circulation 2005;112:2169–74.
5. Kontos MC, Dilsizian V, Weiland F, et al. Iodofiltic acid I 123 (BMIPP) fatty acid imaging improves initial diagnosis in emergency department patients with suspected acute coronary syndromes: a multicenter trial. J Am Coll Cardiol 2010;56:290–9.
6. Nekolla SG, Reder S, Saraste A, et al. Evaluation of the novel myocardial perfusion positron-emission tomography tracer 18F-BMS-747158-02: comparison to 13N-ammonia and validation with microspheres in a pig model. Circulation 2009;119:2333–42.
7. Beller GA, Watson DD. A welcomed new myocardial perfusion imaging agent for positron emission tomography. Circulation 2009;119:2299–301.
8. Spuentrup E, Ruhl KM, Botnar RM, et al. Molecular magnetic resonance imaging of myocardial perfusion with EP-3600, a collagen-specific contrast agent: initial feasibility study in a swine model. Circulation 2009;119:1768–75.
9. Prompona M, Cyran C, Nikolaou K, et al. Contrast-enhanced whole-heart MR coronary angiography at 3.0 T using the intravascular contrast agent gadofosveset. Invest Radiol 2009;44:369–74.

10. Snyder CJ, DelaBarre L, Metzger GJ, et al. Initial results of cardiac imaging at 7 Tesla. Magn Reson Med 2009; 61:517–24.
11. Dewey M, Zimmermann E, Deissenrieder F, et al. Noninvasive coronary angiography by 320-row computed tomography with lower radiation exposure and maintained diagnostic accuracy: comparison of results with cardiac catheterization in a head-to-head pilot investigation Circulation. 2009; 120:867–75.
12. de Graaf FR, Schuijf JD, van Velzen JE, et al. Diagnostic accuracy of 320-row multidetector computed tomography coronary angiography in the non-invasive evaluation of significant coronary artery disease. Eur Heart J 2010;31:1908–15.
13. Achenbach S, Marwan M, Schepis T, et al. High-pitch spiral acquisition: a new scan mode for coronary CT angiography J Cardiovasc Comput Tomogr 2009;3:117–21.
14. Lell M, Marwan M, Schepis T, et al. Prospectively ECG-triggered high-pitch spiral acquisition for coronary CT angiography using dual source CT: technique and initial experience. Eur Radiol 2009;19:2576–83.
15. Hausleiter J, Bischoff B, Hein F, et al. Feasibility of dual-source cardiac CT angiography with high-pitch scan protocols. J Cardiovasc Comput Tomogr 2009;3:236–42.
16. Leschka S, Stolzmann P, Desbiolles L, et al. Diagnostic accuracy of high-pitch dual-source CT for the assessment of coronary stenoses: first experience. Eur Radiol 2009;19:2896–903.
17. Achenbach S, Marwan M, Ropers D, et al. Coronary computed tomography angiography with a consistent dose below 1 mSv using prospectively electrocardiogram-triggered high-pitch spiral acquisition. Eur Heart J 2010;31:340–6.
18. Ishii K, Imai M, Suyama T, et al. Exercised-induced post-ischemic left ventricular delayed reaction or diastolic stunning: is it a reliable marker in detecting coronary artery disease? J Am Col Cardiol 2009;53: 698–705.
19. Senior R, Monaghan M, Main ML, et al. Detection of coronary artery disease with perfusion stress echocardiography using a novel ultrasound imaging agent: two Phase 3 international trials in comparison with radionuclide perfusion imaging. Eur J Echocardiogr 2009;10: 26–35.
20. Hajjiri MM, Leavitt MB, Zheng H, Spooner AE, Fischman AJ, Gewirtz H. Comparison of positron emission tomography measurement of adenosine-stimulated absolute myocardial blood flow versus relative myocardial tracer content for physiological assessment of coronary artery stenosis severity and location. J Am Coll Cardiol Img 2009;2:751–8.
21. Camici PG. Absolute figures are better than percentages. J Am Coll Cardiol Img 2009;2:759–60.
22. Sharir T, Ben-Haim S, Merzon K, et al. High-speed myocardial perfusion imaging: initial clinical comparison with conventional dual detector anger camera imaging. J Am Coll Cardiol Img 2008;1:156–63.
23. Sharir T, Slomka PJ, Hayes SW, et al. Multicenter trial of high-speed versus conventional single-photon emission computed tomography imaging. J Am Coll Cardiol 2010;55:1965–74.
24. Dilsizian V, Narula J. Qualitative and quantitative scrutiny by regulatory process: is the truth subjective or objective? J Am Coll Cardiol Img 2009; 2:1037–8.
25. Watkins S, McGeoch R, Lyne J, et al. Validation of magnetic resonance myocardial perfusion imaging with fractional flow reserve for the detection of significant coronary heart disease. Circulation 2009;120: 2207–13.
26. Bernhardt P, Spiess J, Levenson B, et al. Combined assessment of myocardial perfusion and late gadolinium enhancement in patients after percutaneous coronary intervention or bypass grafts: a multicenter study of an integrated cardiovascular magnetic resonance protocol. J Am Coll Cardiol Img 2009;2:1292–300.
27. Yang Q, Li K, Liu X, et al. Contrast-enhanced whole-heart coronary magnetic resonance angiography at 3.0-T: a comparative study with X-ray angiography in a single center. J Am Coll Cardiol 2009;54:69–76.
28. Hadamitzky M, Freissmuth B, Meyer T, et al. Prognostic value of coronary computed tomographic angiography for prediction of cardiac events in patients with suspected coronary artery disease. J Am Coll Cardiol Img 2009;2:404–11.
29. Chow BJ, Wells GA, Chen L, et al. Prognostic value of 64-slice cardiac computed tomography severity of coronary artery disease, coronary atherosclerosis, and left ventricular ejection fraction. J Am Coll Cardiol 2010;55: 1017–28.
30. Hoffmann U, Bamberg F, Chae CU, et al. Coronary computed tomography angiography for early triage of patients with acute chest pain: the ROMICAT (Rule Out Myocardial Infarction using Computer Assisted Tomography) trial. J Am Coll Cardiol 2009;53:1642–50.
31. Hollander JE, Chang AM, Shofer FS, et al. One-year outcomes following coronary computerized tomographic angiography for evaluation of emergency department patients with potential acute coronary syndrome. Acad Emerg Med 2009;16:693–8.
32. Min JK, Shaw LJ, Berman DS. The present state of coronary computed tomography angiography a process in evolution. J Am Coll Cardiol 2010;55: 957–65.
33. Min JK, Gilmore A, Budoff MJ, Berman DS, O'Day K. Cost-effectiveness of coronary CT angiography versus myocardial perfusion SPECT for evaluation of patients with chest pain and no known coronary artery disease. Radiology 2010;254:801–8.
34. Halpern EJ, Savage MP, Fischman DL, Levin DC. Cost-effectiveness of coronary CT angiography in evaluation of patients without symptoms who have positive stress test results. AJR Am J Roentgenol 2010;194: 1257–62.
35. Ladapo JA, Jaffer FA, Hoffmann U, et al. Clinical outcomes and cost-effectiveness of coronary computed tomography angiography in the evaluation of patients with chest pain. J Am Coll Cardiol 2009;54:2409–22.
36. Abidov A, Gallagher MJ, Chinnaiyan KM, Mehta LS, Wegner JH, Raff GL. Clinical effectiveness of coronary computed tomographic angiography in the triage of patients to cardiac catheterization and revascularization after inconclusive stress testing: results of a 2-year prospective trial. J Nucl Cardiol 2009;16:701–13.
37. May JM, Shuman WP, Strote JN, et al. Low-risk patients with chest pain in the emergency department: negative 64-MDCT coronary angiography may reduce length of stay and hospital charges. AJR 2009;193:150–4.
38. Schepis T, Achenbach S, Marwan M, et al. Prevalence of first-pass myocardial perfusion defects detected by contrast-enhanced dual-source CT in patients with non-ST segment elevation acute coronary syndromes. Eur Radiol 2010;20:1607–14.
39. Blankstein R, Shturman LD, Rogers IS, et al. Adenosine-induced stress myocardial perfusion imaging using dual-source cardiac computed tomography. J Am Coll Cardiol 2009;54: 1072–284.
40. George RT, Arbab-Zadeh A, Miller JM, et al. Adenosine stress 64- and 256-row detector computed tomography angiography and perfusion imaging: a pilot study evaluating the transmural extent of perfusion abnormalities to predict atherosclerosis causing myocardial ischemia. Circ Cardiovasc Imaging 2009;2:174–82.

41. Okada DR, Ghoshhajra BB, Blankstein R, et al. Direct comparison of rest and adenosine stress myocardial perfusion CT with rest and stress SPECT. J Nucl Cardiol 2010;17:27–37.
42. Rocha-Filho JA, Blankstein R, Shturman LD, et al. Incremental value of adenosine-induced stress myocardial perfusion imaging with dual-source CT at cardiac CT angiography. Radiology 2010;254:410–9.
43. Kim HW, Farzaneh-Far A, Kim RJ. Cardiovascular magnetic resonance in patients with myocardial infarction: current and emerging applications. J Am Coll Cardiol 2009;55:1–16.
44. Mewton N, Croisille P, Gahide G, et al. Effect of cyclosporine on left ventricular remodeling after reperfused myocardial infarction. J Am Coll Cardiol 2010;55:1200–5.
45. Atar D, Petzelbauer P, Schwitter J, et al. Effect of intravenous FX06 as an adjunct to primary percutaneous coronary intervention for acute ST-segment elevation myocardial infarction: results of the F.I.R.E. (Efficacy of FX06 in the Prevention of Myocardial Reperfusion Injury) trial. J Am Coll Cardiol 2009;53:720–9.
46. Lonborg J, Kelbaek H, Vejlstrup N, et al. Cardioprotective effects of ischemic postconditioning in patients treated with primary percutaneous coronary intervention, evaluated by magnetic resonance. Circ Cardiovasc Interv 2010;3:34–41.
47. Ichikawa Y, Kitagawa K, Chino S, et al. Adipose tissue detected by multislice computed tomography in patients after myocardial infarction. J Am Coll Cardiol Img 2009;2:548–55.
48. Hedstrom E, Engblom H, Frogner F, et al. Infarct evolution in man studied in patients with first-time coronary occlusion in comparison to different species—implications for assessment of myocardial salvage. J Cardiovasc Magn Reson 2009;11:38.
49. Roes SD, Mollema SA, Lamb HJ, van der Wall EE, de Roos A, Bax JJ. Validation of echocardiographic two-dimensional speckle tracking longitudinal strain imaging for viability assessment in patients with chronic ischemic left ventricular dysfunction and comparison with contrast-enhanced magnetic resonance imaging. Am J Cardiol 2009;104:312–7.
50. Peteiro J, Bouzas-Mosquera A, Broullon FJ, Garcia-Campos A, Pazos P, Castro-Bieras A. Prognostic value of peak and post-exercise treadmill exercise echocardiography in patients with known or suspected coronary artery disease. Eur Heart J 2010;31:187–95.
51. Bouzas-Mosquera A, Peteiro J, Alvarez-Garcia N, et al. Prediction of mortality and major cardiac events by exercise echocardiography in patients with normal exercise electrocardiographic testing. J Am Col Cardiol 2009;53:1981–90.
52. Stanton T, Ingul CB, Hare J, Leano R, Marwick T. Association of myocardial deformation with mortality independent of myocardial ischemia and left ventricular hypertrophy. J Am Col Cardiol Img 2009;2:793–801.
53. Soman P, Udelson JE. Gated SPECT myocardial perfusion imaging for the prediction of incident heart failure: an old dog learns a new trick. J Am Coll Cardiol Img 2009;1401–3.
54. Nakata T, Hashimoto A, Wakabayashi T, Kusuoka H, Nishimura T. Prediction of new-onset refractory congestive heart failure using gated myocardial perfusion SPECT imaging in patients with known or suspected coronary artery disease. J Am Coll Cardiol Img 2009;2:1393–400.
55. Hachamovitch R, Kang X, Amanullah AM, et al. Prognostic implications of myocardial perfusion single-photon emission computed tomography in the elderly. Circulation 2009;120:2197–206.
56. Chang SM, Nabi F, Xu J, Raza U, Mahmarian JJ. Normal stress-only versus standard stress/rest myocardial perfusion imaging. J Am Coll Cardiol 2010;55:221–30.
57. Herzog BA, Husmann L, Valenta I, et al. Long-term prognostic value of 13N-ammonia myocardial perfusion positron emission tomography. J Am Coll Cardiol 2009;54:150–6.
58. Dilsizian V, Bacharach SL, Beanlands SR, et al. PET myocardial perfusion and metabolism clinical imaging. J Nucl Card 2009;16:651.
59. Kim HW, Klem I, Shah DJ, et al. Unrecognized non-Q-wave myocardial infarction: prevalence and prognostic significance in patients with suspected coronary disease. PLoS Med 2009;6:e1000057.
60. Cheong BYC, Muthupillai R, Wilson JM, et al. Prognostic significance of delayed-enhancement magnetic resonance imaging: survival of 857 patients with and without left ventricular dysfunction. Circulation 2009;120:2069–76.
61. Kwon Dh, Halley CM, Carrigan TP, et al. Extent of left ventricular scar predicts outcomes in ischemic cardiomyopathy patients with significantly reduced systolic function: a delayed hyperenhancement cardiac magnetic resonance study. J Am Coll Cardiol Img 2009;2:34–44.
62. Rahimi K, Banning AP, Cheng ASH, et al. Prognostic value of coronary revascularisation-related myocardial injury: a cardiac magnetic resonance imaging study. Heart 2009;95:1937–43.
63. Blaha M, Budoff MJ, Shaw LJ, et al. Absence of coronary artery calcification and all-cause mortality. J Am Coll Cardiol Img 2009;2:692–700.
64. Budoff MJ, McClelland RL, Nasir K, et al. Cardiovascular events with absent or minimal coronary calcification: the Multi-Ethnic Study of Atherosclerosis (MESA). Am Heart J 2009;158:554–61.
65. Sarwar A, Shaw LJ, Shapiro MD, et al. Diagnostic and prognostic value of absence of coronary artery calcification. J Am Coll Cardiol Img 2009;2:675–88.
66. Min JK, Lin FY, Gidseg DS, et al. Determinants of coronary calcium conversion among patients with a normal coronary calcium scan: what is the "warranty period" for remaining normal? J Am Coll Cardiol 2010;55:1110–7.
67. van Werkhoven JM, Schuijf JD, Gaemperli O, et al. Incremental prognostic value of multi-slice computed tomography coronary angiography over coronary artery calcium scoring in patients with suspected coronary artery disease. Eur Heart J 2009;30:2622–9.
68. Uetani T, Amano T, Kunimura A, et al. The association between plaque characterization by CT angiography and post-procedural myocardial infarction in patients with elective stent implantation. J Am Coll Cardiol Img 2010;3:19–28.
69. Cheng VY, Dey D, Tamarappoo B, et al. Pericardial fat burden on ECG-gated noncontrast CT in asymptomatic patients who subsequently experience adverse cardiovascular events. J Am Coll Cardiol Img 2010;3:352–60.
70. Abbara S, Arbab-Zadeh A, Callister TQ, et al. SCCT guidelines for performance of coronary computed tomographic angiography: a report of the Society of Cardiovascular Computed Tomography Guidelines Committee. J Cardiovasc Comput Tomogr 2009;3:190–204.
71. Raff GL, Abidov A, Achenbach S, et al. Society of Cardiovascular Computed Tomography. SCCT guidelines for the interpretation and reporting of coronary computed tomographic angiography. J Cardiovasc Comput Tomogr 2009;3:122–36.
72. Hundley WG, Bluemke D, Bogaert J, et al. Society for Cardiovascular Magnetic Resonance guidelines for reporting cardiovascular magnetic resonance examinations. J Cardiovasc Magn Reson 2009;11:5.

73. Mark DB, Berman DS, Budoff MJ, et al. ACCF/ACR/AHA/NASCI/SAIP/SCAI/SCCT 2010 expert consensus document on coronary computed tomographic angiography: a report of the American College of Cardiology Foundation Task Force on Expert Consensus Documents. J Am Coll Cardiol 2010;55:2663–99.
74. Hundley WG, Bluemke DA, Finn JP, et al. American College of Cardiology Foundation Task Force on Expert Consensus Documents. ACCF/ACR/AHA/NASCI/SCMR 2010 expert consensus document on cardiovascular magnetic resonance: a report of the American College of Cardiology Foundation Task Force on Expert Consensus Documents. J Am Coll Cardiol 2010;55:2614–62.
75. Hendel RC, Berman DS, Di Carli MF, et al. ACCF/ASNC/ACR/AHA/ASE/SCCT/SCMR/SNM 2009 appropriate use criteria for cardiac radionuclide imaging: a report of the American College of Cardiology Foundation Appropriate Use Criteria Task Force, the American Society of Nuclear Cardiology, the American College of Radiology, the American Heart Association, the American Society of Echocardiography, the Society of Cardiovascular Computed Tomography, the Society for Cardiovascular Magnetic Resonance, and the Society of Nuclear Medicine. J Am Coll Cardiol 2009;53:2201–29.

Key Words: cardiac magnetic resonance ■ computed tomography ■ coronary artery disease ■ echocardiography ■ nuclear imaging.